INL/CON-10-18046
PREPRINT

The Role of Environment on High Temperature Creep-Fatigue Behavior of Alloy 617

ASME PVP 2010

Laura Carroll
Celine Cabet
Richard Wright

July 2010

The INL is a
U.S. Department of Energy
National Laboratory
operated by
Battelle Energy Alliance

Proceedings of the ASME 2010 Pressure Vessel and Piping Division Conference
PVP2010
July 18-22, 2010, Bellevue, Washington, USA

PVP2010-26126

THE ROLE OF ENVIRONMENT ON HIGH TEMPERATURE CREEP-FATIGUE BEHAVIOR OF ALLOY 617

Laura Carroll
Idaho National Laboratory
Idaho Falls, ID, USA

Celine Cabet
CEA, DEN, DPC, SCCME
Gif-sur-Yvette, France

Richard Wright
Idaho National Laboratory
Idaho Falls, ID, USA

ABSTRACT

Alloy 617 is the leading candidate material for an intermediate heat exchanger (IHX) application of the Very High Temperature Nuclear Reactor (VHTR), expected to have an outlet temperature as high as 950°C. Acceptance of Alloy 617 in Section III of the ASME Code for nuclear construction requires a detailed understanding of the creep-fatigue behavior. Initial creep-fatigue work on Alloy 617 suggests a more dominant role of environment with increasing temperature and/or hold times evidenced through changes in creep-fatigue crack growth mechanism/s and failure life. Furthermore, previous work on corrosion of nickel base alloys in impure helium has suggested that this environment is far from inert with respect to Alloy 617. Continuous cycle fatigue and creep-fatigue testing of Alloy 617 was conducted at 950°C and 0.3% and 0.6% total strain in air to simulate damage modes expected in a VHTR application. Continuous cycle and creep-fatigue specimens exhibited intergranular cracking, but did not show evidence of grain boundary cavitation. Despite the absence of grain boundary cavitation to accelerate crack propagation, the addition of a hold time at peak tensile strain was detrimental to cycle life. This suggests that creep-fatigue interaction may occur by a different mechanism or that the environment may be partially responsible for accelerating failure.

INTRODUCTION

The Next Generation Nuclear Plant (NGNP) being developed in the US is a Very High Temperature Nuclear Reactor (VHTR) with a gas as the primary coolant. Conceptual design requires an outlet temperature of greater than 850°C to efficiently generate hydrogen, with a maximum expected temperature of 950°C. A critical component in the VHTR system is the Intermediate Heat Exchanger (IHX), which will operate at the reactor outlet temperature of up to 950°C. Helium is the VHTR cooling gas and is expected to contain low levels of residual impurities that can react with the high temperature materials causing corrosion. The combination of very high temperature operation and long duration of service requires structural materials with good thermal stability as well as high temperature creep and oxidation resistance. Based on these material requirements, the nickel base alloy UNS N06617, Alloy 617, is the leading IHX candidate alloy. Alloy 617 is strengthened by solid solution hardening provided by the alloy elements chromium, cobalt and molybdenum as well as by intra- and inter-granular carbide precipitates. The high temperature oxidation resistance is derived from the high nickel and chromium content.

Alloy 617 is approved for non-nuclear construction in ASME Code Section I and Section VIII, Division 1 but is not currently qualified for nuclear use in ASME Code Section III. A draft Code case was developed in the 1980's to qualify the alloy for nuclear service but efforts were stopped before the approval process was completed. A review of the mechanical property database developed for the draft case identified the need for complementary creep-fatigue data on the base metal and weldments. Additionally, Nuclear Regulatory Commission (NRC) licensing of a high temperature reactor will likely require an understanding of the environmental effects of impure helium on creep-fatigue. Creep-fatigue deformation is expected to be the primary damage mode for the IHX occurring as transients during start up and shut down produce cyclic loadings, while the stresses relax during steady power operation inducing creep damage.

Creep-fatigue testing, strain controlled fatigue with a hold time, is performed in a laboratory setting to reproduce the expected damage mode. Previous work has found for Alloy 617 that a hold time during the tensile portion of the fatigue cycle is more damaging than compressive holds or both a tensile and compressive hold (1-3). It is difficult to separate

the effects of temperature, strain range, strain rate and environment as they have complex interrelationships. Nagato and coworkers observed that the fatigue life of Hastelloy X, a nickel base alloy rich in Cr, was longer in impure helium than in air but the effect of environment was less remarkable at temperatures above 800°C and for creep-fatigue (4). At temperatures of 750°, 850° and 950°C, Meurer and coworkers observed a slight increase in the fatigue life of Alloy 617 tested in impure helium compared to air at a total strain of 0.3%; this difference was not evidenced at higher strain ranges (3). Strizak and coworkers concluded that a helium environment was not detrimental to fatigue life of Alloy 617 at temperatures of up to 704°C (5) and Rao and coworkers concluded that at 950°C the influence of environment, if any, is strongly reduced for longer hold times (1). The results of previous studies of the creep-fatigue behavior in a helium environment have been inconclusive and the relationship between environment, mechanism, and microstructural evolution has not been investigated in detail. The influence of the strain rate on the creep-fatigue lifetime was not conclusive (1-2, 4) and it is also unclear whether the influence of the hold time does (6) or doesn't saturate (1-2) at long hold times. These apparent discrepancies may be attributed to changes in the failure mode with variations in the test parameters and is a major drawback to modeling of the creep-fatigue interaction.

To address the needs of VHTR IHX materials, a comprehensive program was launched to assess the creep-fatigue resistance of Alloy 617. The long term goal is to determine the influence of the environment (temperature, strain rate, and atmosphere) on the creep-fatigue life of Alloy 617. The fatigue and creep-fatigue behavior of Alloy 617 is initially investigated in air at 950°C at 0.3% and 0.6% total strain ranges. Future work will include testing in a VHTR controlled helium environment and comparison of the fatigue mechanisms observed in air and in impure helium. After testing, microstructural evaluation was completed to develop an understanding of the fatigue and creep-fatigue data through changes in the surface and bulk microstructure as well as in the crack failure mode.

EXPERIMENTAL PROCEDURE

Low cycle fatigue and creep-fatigue testing was conducted on Alloy 617, the composition of which is given in Table I.

TABLE I – ALLOY 617 COMPOSITION (HEAT XX2834UK) IN WT%

Ni	C	Cr	Co	Mo	Fe	Al	Ti	
bal	0.08	21.9	11.4	9.3	1.7	1.0	0.3	Si:0.1; Mn: 0.1 Cu: 0.04

The alloy microstructure is shown in Figure 1. Cylindrical creep-fatigue specimens, 7.5 mm diameter in the reduced section and a gage length of 12 mm, were machined from annealed plate; the long axis of the specimen aligned with the rolling direction. Low stress grinding was used during the final machining. The fatigue specimens were machined at Metcut Research, LLC. and testing was performed at Idaho National Laboratory (INL) in accordance with ASTM Standard E606-04 (7).

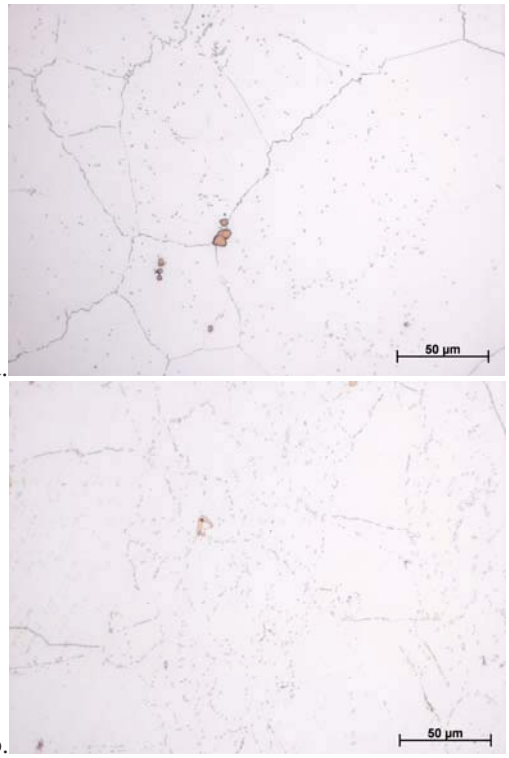

FIG. 1 – MICROSTRUCTURE OF THE (A) AS-ANNEALED AND (B) AGED ALLOY 617 (AGING FOR 200H AT 950°C)

Low cycle fatigue and creep-fatigue testing was conducted on MTS Systems Corporation Model 810 servo-hydraulic test machines in axial strain-control mode. In all cases, radio-frequency induction heating was used to heat the specimens. The temperature gradient was measured with a specimen instrumented with spot-welded thermocouples along the gage length and was found to deviate by less than 1% within the gage section. Temperature control was achieved using a combination of spot-welded thermocouples on the shoulder of the specimen and a thermocouple loop at the center of the gage section.

Fully reversed strain controlled low cycle fatigue and creep-fatigue testing was completed at a 0.3% and a 0.6% total strain range at 950°C. A triangular waveform and a ramp rate of 10^{-3} /sec were used for low cycle fatigue testing. Creep-fatigue testing followed the described strain waveform except that a tensile hold, of 18 sec to as long as 1800 sec (30 min), was imposed at the maximum tensile strain. Tests were controlled using the MTS Systems Corporation software, MPT Testware. Several data collection schemes were implemented to fully characterize the hysteresis loops and peak/valley strains and stresses. An interleaved time and strain data collection records data at a specified change in time or strain. This type

of data was collected initially from every cycle and then for cycles at a decreasing frequency with increasing cycle count. Peak and valley tensile and compressive strains (and stresses) were also recorded for each cycle.

In all cases, a step to strain approach was used during the first 7 cycles. The target strain was gradually increased until the 8th cycle in which the peak strains were reached. This technique was used to avoid exceeding the desired strain in the first cycles, which typically occurs for Alloy 617 at very high temperatures.

The number of cycles to macro-crack initiation, N_0, and the number of cycles to failure, N_{20}, were defined as the point at which the ratio of the peak tensile stress to the peak compressive stress initially declined and the point at which the ratio was 80% of its stable value, respectively (8). Test termination was prior to actual specimen separation. Additional detail regarding this failure life criterion is given in the referenced article (8).

Upon completion of a test, the test was switched into load control and the load was brought to zero before the specimen was cooled. In some cases, the failed specimen may have remained at high temperature for some time prior to cooling to room temperature. Specimens were removed from the load frame, cut and mounted in epoxy with alumina particles for edge retention such that the long axis or stress direction was in the plane of the mount surface for a two dimensional view of the gage section. The mounts were electro-etched at 2 volts in a solution of 5% oxalic acid to create a lightly etched surface. It was found that overetching the specimens resulted in grain boundary pitting thus a light etch was critical to the microstructural analysis. Optical and scanning electron microscopy with EDS analysis was then conducted.

RESULTS

Low Cycle Fatigue Behavior

Continuous low cycle fatigue (LCF) testing was completed in air at 950°C to provide a baseline for the creep-fatigue behavior. Table II lists the test conditions. Two strain ranges were investigated, 0.3% and 0.6% total strain. The number of cycles to failure, inelastic strain at a midlife cycle, and the total test time are also included in Table II.

Table II – Fatigue and creep-fatigue tests completed at 950°C and a strain rate of 10^{-3}/sec

Total Strain Range (%)	Hold Time (min)	Cycles to Initiation (N_0)	Cycles to Failure (N_{20})	Time to Failure (hours)	Inelastic Strain Range @ Midlife (%)
0.3	0	8639	9641	16	0.102
0.3	0	5033	5867	9	0.105
0.3	0	8139	9000	15	0.084
0.3	3	2600	3989	206	0.202
0.3	3	1944	2485	128	0.212
0.3	10	3583	4096	689	0.199
0.3	10	3569	4430	745	0.200
0.6	0	783	1722	6	0.436
0.6	0	762	1390	5	0.441
0.6	0	826	1480	5	0.441
0.6	3	450	950	51	0.488
0.6	3	297	922	49	0.503
0.6	10	402	686	117	0.510
0.6	10	416	634	108	0.506
0.6	30	367	661	333	0.524

The peak tensile and compressive stresses observed in the LCF tests at 0.3% and 0.6% total strain were relatively symmetrical, i.e. the peak tensile and compressive stresses were of the same magnitude, as shown in Figure 2(a) and 3(a), respectively. Furthermore, a steady state stress was reached in approximately 10 cycles and remained constant until macrocrack initiation or just prior to failure. For the 0.6% total strain tests, the peak stresses of the initial cycles were greater in magnitude than the steady state stress despite the fact that the peak strains had not yet reached the target test strain. Also, note that the steady state peak stress in the 0.6% total strain test was similar in magnitude to the 0.3% total strain test. This is consistent with the shape of the hysteresis loops shown in Figures 2(b) and 3(b) for the 0.3% and 0.6% total strain conditions, respectively. The hysteresis loops were relatively unchanging for cycles 9, 99, and 999 and thus the inelastic strain also did not change significantly as a function of cycle.

Creep-Fatigue Behavior

Creep-fatigue testing was also conducted at 950°C in air with tensile hold times of up to 1800 sec. A list of the creep-fatigue conditions and the baseline fatigue data is shown in Table II; total test times were as long as 1 month.

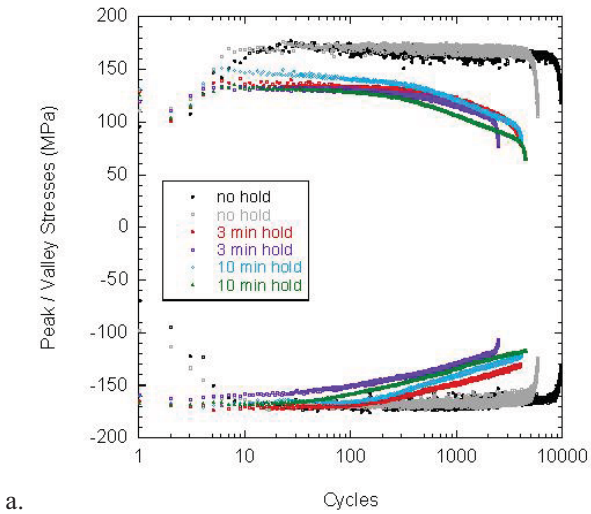

a.

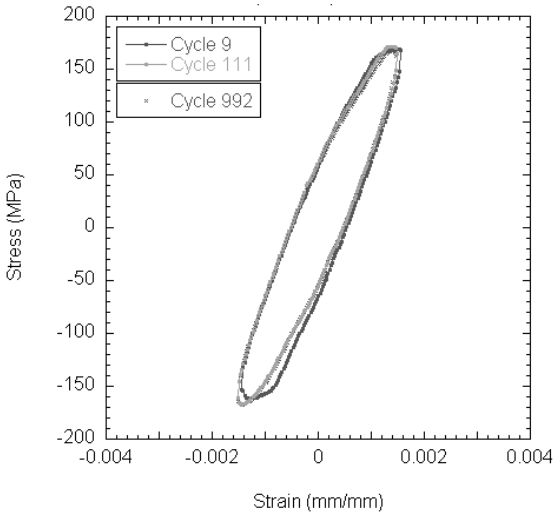

b.

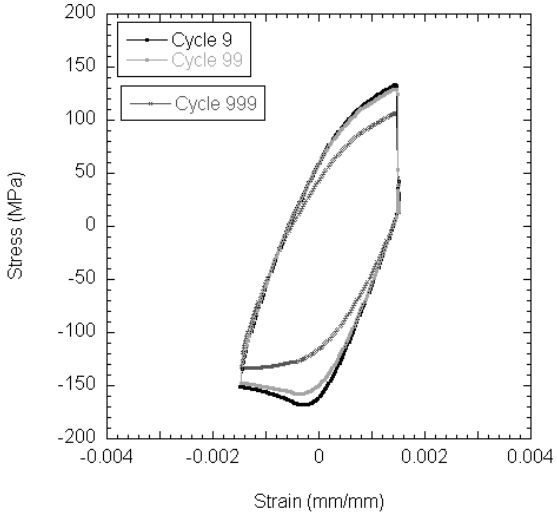

c.

FIG. 2 – PEAK TENSILE AND COMPRESSIVE STRESS PLOTTED AS A FUNCTION OF CYCLE FOR CREEP-FATIGUE TESTS AT 950°C AND A 0.3% TOTAL STRAIN RANGE (A). HYSTERESIS LOOPS FOR THE NO HOLD (B) AND 10 MIN HOLD (C) CREEP-FATIGUE TEST SHOWN FOR SELECTED CYCLES

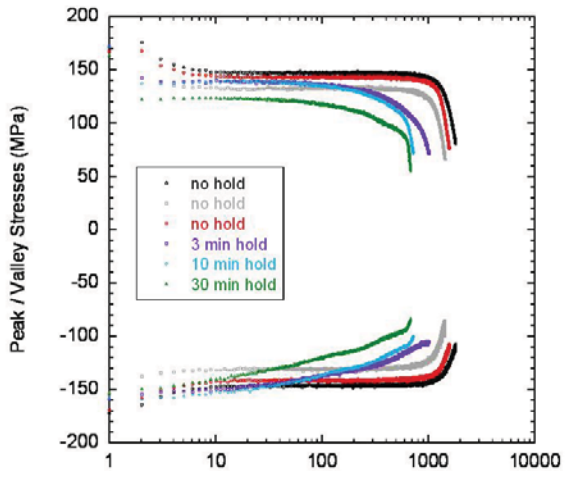

a.

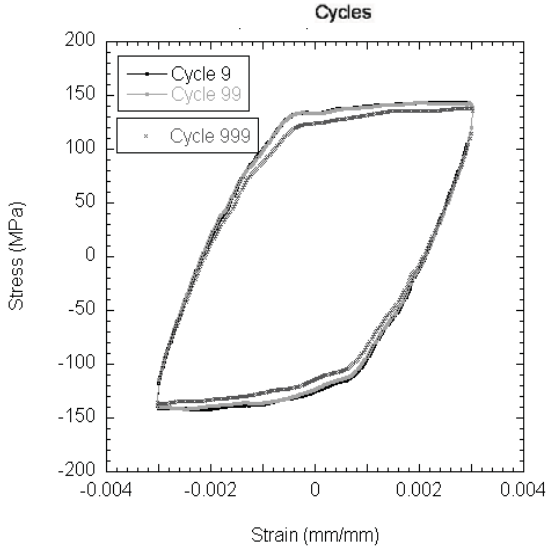

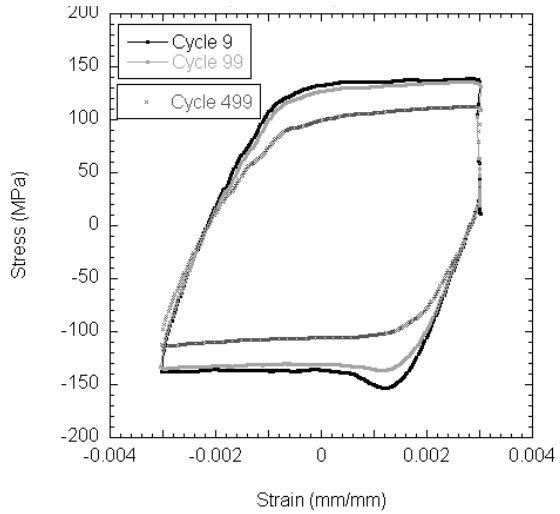

FIG. 3 – PEAK TENSILE AND COMPRESSIVE STRESS PLOTTED AS A FUNCTION OF CYCLE FOR CREEP-FATIGUE TESTS AT 950°C AND A 0.6% TOTAL STRAIN RANGE (A). HYSTERESIS LOOPS FOR THE NO HOLD (B) AND 10 MIN HOLD (C) CREEP-FATIGUE TEST SHOWN FOR SELECTED CYCLES

The peak tensile and compressive stresses are also shown as a function of cycle for the creep-fatigue tests, as shown in Figures 2(a) and 3(a). The creep-fatigue peak stresses versus cycle profiles were similar regardless of the duration of the tensile hold. The peak stresses did not achieve a steady state value, instead the peak stresses slowly decreased with cycle and had two transition points following which a more rapid decrease was observed. The creep-fatigue peak stresses versus cycle profiles were also relatively symmetric, although the magnitude of the stresses in compression were slightly greater than in tension. The peak stresses in the longer hold time tests were also slightly lower with increasing hold time, however, there was some degree of variability in the peak stresses for identical test conditions. The hysteresis loops shown in Figure 2(c) and Figure 3(c) illustrate the decreasing magnitude of the peak stresses at later cycles. The loops shown for cycles 499 and 999 illustrate this lower peak stress magnitude, although the width of the loops at zero strain, the inelastic strain, did not vary greatly.

The number of cycles to failure decreased with increasing tensile hold times for both strain ranges, as shown in Figure 4. Lines are shown on the plot but are not meant to accurately capture the trend with hold time.

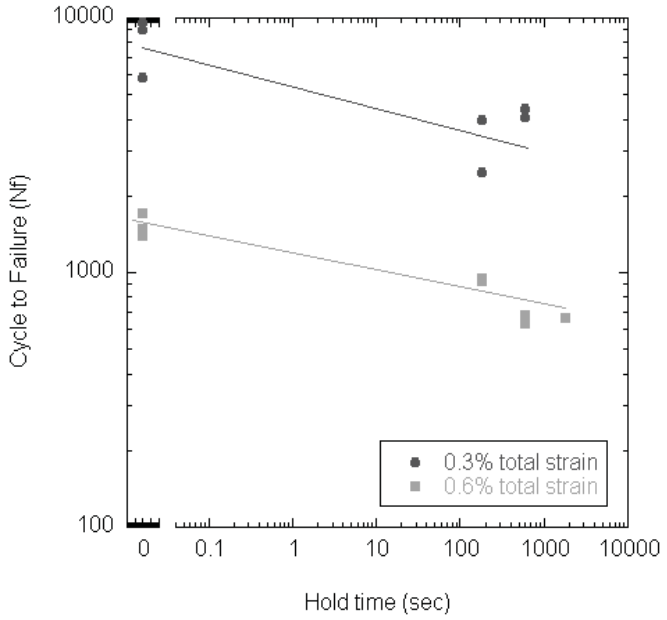

FIG. 4 – CYCLES TO FAILURE AS A FUNCTION OF HOLD TIME FOR CREEP-FATIGUE TESTING AT 950°C

In the case of the 0.3% total strain range, the addition of a 3 minute hold time reduced the number of cycles to failure by a factor of 2. An increase in hold time to 10 minutes did not further reduce the cycle life. At the 0.6% total strain range, increasing the hold time to 10 minutes caused increasing reductions in the cycles to failure, although the 30 minute hold time test did not further reduce the creep-fatigue life. Due to the variability observed in fatigue and creep-fatigue additional data is necessary.

Stress relaxation curves are shown for both strain ranges for creep-fatigue tests with a 180 sec and 600 sec hold time in Figure 5. At both strain ranges, the stress relaxation during the hold period at constant strain occurred at the same rate for the 180 sec and the 600 sec hold. Initially the stress decreased rapidly until approximately 60 sec into the hold. The creep rate may be calculated from the slope of these curves and the elastic modulus. The creep rate in the 0.6% total strain, 10 minute hold test is approximately 10^{-7} /sec. This rate was calculated using the slope from 100 sec into the hold until 600 sec. The creep rate is on the order of 10^{-8} /sec during the hold period in the 0.3% total strain, 10 minute hold creep-fatigue test.

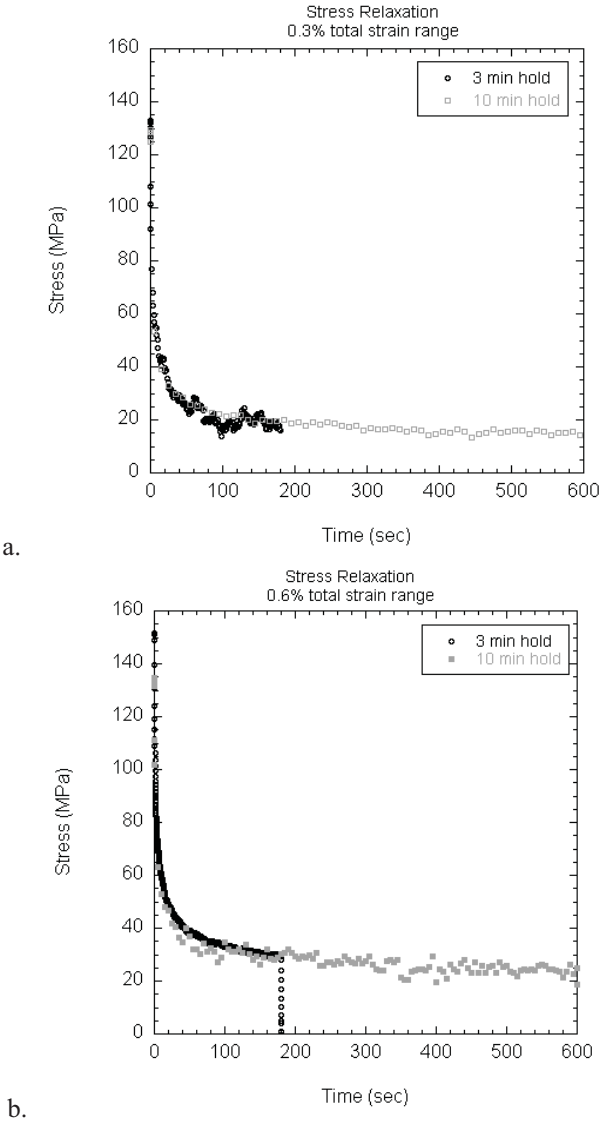

FIG. 5 – STRESS RELAXATION CURVES FOR CREEP-FATIGUE TESTS AT 950°C AND 0.3% (A) AND 0.6% (B) TOTAL STRAIN RANGE

Microstructure and failure mode

The creep-fatigue specimens bulged in the center of the gage section prior to or upon failure. This was not observed for continuously cycled specimen, as shown in Figure 6 for a fatigue and creep-fatigue specimens tested at a total strain range of 0.3%. Bulging in creep-fatigue specimens tested with a peak tensile hold was also observed by Rao and coworkers (1). The failed specimen surfaces have a green color, typical of chromium oxide. The surface layer of the LCF specimen appears to be thin and traces of the grain boundaries are visible through the surface oxide (exposure for 16 hours at 950°C). The creep-fatigue specimen shown in Figure 6(b) spent approximately 700 hours at 950°C.

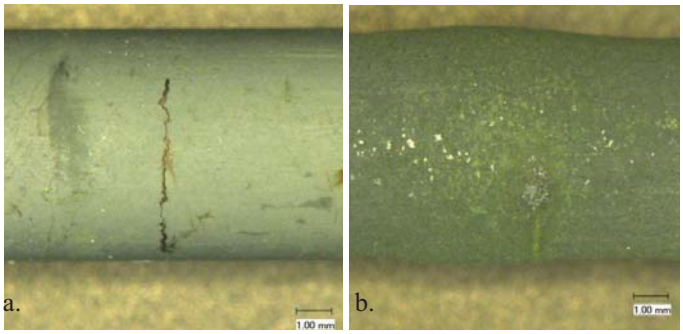

Fig. 6 – Specimen tested at a total strain range of 0.3% in low cycle fatigue (a) and creep-fatigue with a 10 min hold (b). The creep-fatigue specimens bulged in the center of the gage section prior to or upon failure. This was not observed when a hold time was not included in the cycle

In continuous cycling tests at both strain ranges, the cracks initiated and propagated in a predominantly intergranular manner. Figure 7(a) shows a longitudinal cross section through the specimen gage section after LCF testing at 0.6% total strain. The stress axis is from left to right in the plane of the page. The edges of the cracks were slightly oxidized and there was little indication of an oxide having formed on the surface of the specimen, as shown in Figure 8(a). EDS analysis identified that the edges of the cracks were mainly covered by a chromium oxide rich in titanium. There was a greater degree of surface cracking for the 0.6% strain range specimens than in the specimens tested at a 0.3% total strain.

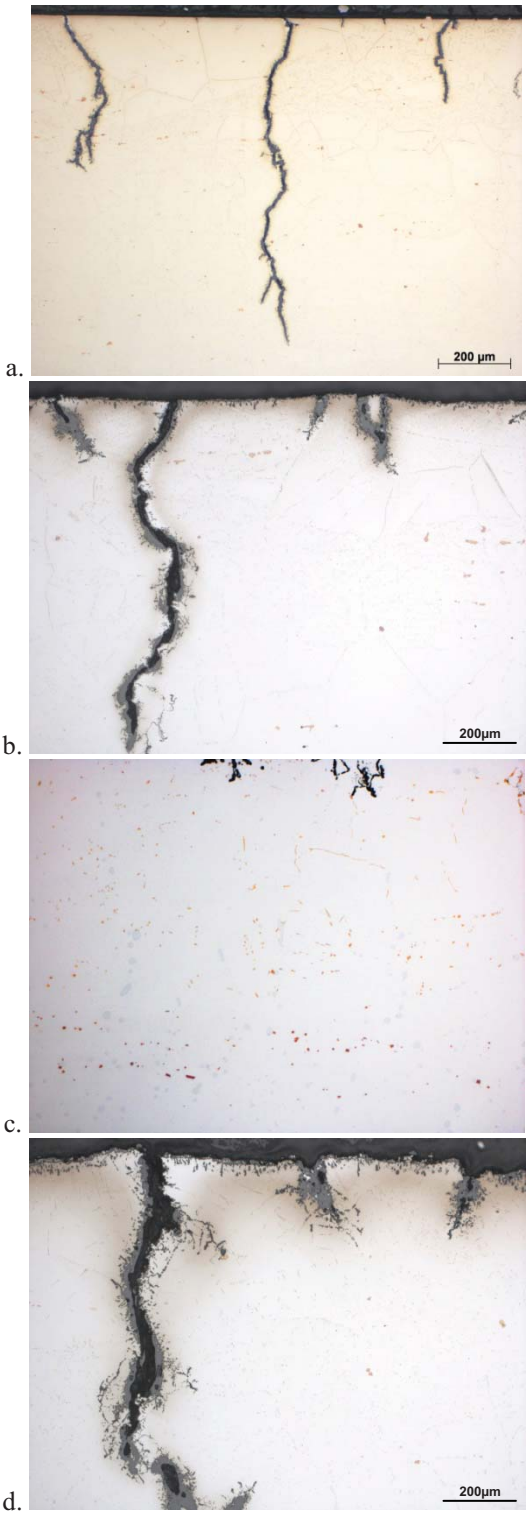

Fig. 7 – Optical images of specimens tested at a total strain range of 0.6% in low cycle fatigue (a) and creep-fatigue with either a 600 sec hold (b and c) and a 1800 sec hold (d). The image in (c) is at a depth of ~1000µm below the specimen surface. The stress axis is from right to left in the plane of the page

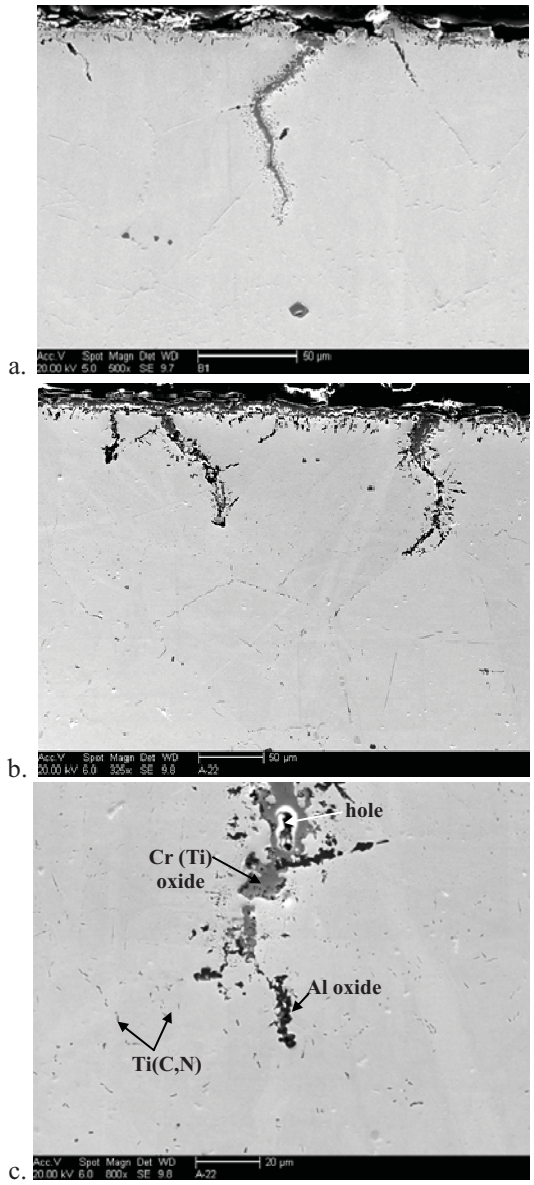

FIG. 8 – SEM IMAGES OF SPECIMENS TESTED AT A TOTAL STRAIN RANGE OF 0.3% IN LOW CYCLE FATIGUE (A) AND CREEP-FATIGUE WITH AN 1800 SEC HOLD (B AND C). THE STRESS AXIS IS FROM RIGHT TO LEFT IN THE PLANE OF THE PAGE

For the specimens tested in creep-fatigue, all of the grain boundaries in contact with the specimen surface were oxidized, as shown in Figures 7(b) and 7(d). A fraction of these intergranular oxide veins have initiated intergranular cracks. The crack propagation was predominantly intergranular. EDS analysis showed that the thin finger-like intergranular oxides were mainly aluminum oxide. Chromium oxide rich in titanium likely formed on the edges when the crack was opened. A chromium oxide scale formed on the specimen surface as well. The cracks were wider for the specimens cycled at a total strain range of 0.6% than those cycled at the lower strain range. Aluminum oxide has formed along the grain boundaries that intersect the crack and those ahead of the crack tip, as shown in Figure 8(c). The regions ahead of the crack tip and in the bulk material did not exhibit either grain boundary cavitation, void formation, or grain boundary cracking typically associated with creep damage.

In addition to the microstructural evolution due to aging at 950°C, fatigue testing induced changes in the precipitation morphology, as shown in Figures 1(b) and 7(c). The most obvious difference associated with the synergetic effect of temperature and load observed in the deformed specimen is the large number of fine precipitates, particularly near the specimen surface and in the vicinity of the cracks.

DISCUSSION

Similar to what has been observed for stainless steels (9-10) and nickel base alloys (1, 11), the introduction of hold times at peak tensile strain in continuous cycle fatigue reduces the fatigue life of Alloy 617, as shown in Figure 4. A greater decrease in cycles to failure at lower strain ranges with increasing hold time was also observed, consistent with the results of Nimonic PE-16, a Ni-Cr superalloy (12). Furthermore, the amount of inelastic strain is relatively similar with increasing hold times, particularly at the 0.6% strain range, as shown in Figures 2 and 3. More data is necessary to illicit the influence of an increasing hold time on cycle life.

The continuous cycle fatigue life observed for Alloy 617, listed in Table I, is similar to that reported for Alloy 617 by Meurer and co-workers (13). The cycle lifetimes are approximately the same for the 0.3% strain range, but the cycles to failure are slightly less at the 0.6% strain range than found in the present work. Rao and coworkers also reported creep-fatigue results for Alloy 617 at the 0.6% total strain range, however this testing was conducted in a simulated nuclear reactor helium environment (1). The continuous cycle lifetimes reported by Rao et al. are slightly higher than those reported here, whereas they are half an order of magnitude greater than those reported by Meurer et al. The creep-fatigue data of Rao et al. is similar to that reported here for the 180 sec tensile hold condition but is slightly less for increasing hold time durations. The differences may be explained by variation among heats of Alloy 617 but may also be due to differences in testing methods and/or definitions of failure. In the case of the data reported by Rao et al., the differences may also be a result of the helium environment.

For continuous cycle fatigue, the peak tensile stresses as a function of cycle reached a stable value within less than 10 cycles at 0.3% total strain and within 5 cycles at 0.6% total strain. The creep-fatigue peak stresses decreased slowly with cycle initially and, in contrast to the continuous cycle fatigue, began to decrease at a cycle relatively early in the test. This softening or peak stress decrease was more significant for the compressive peak stresses than the tensile stresses, as shown in Figure 2. Although the number of cycles to failure decreases

with increasing hold times, the peak stresses are similar for the longer hold time tests, as shown in Figure 2. Also, the tensile and compressive peak stresses were similar in the 0.3% and 0.6% strain range despite the higher strain range of the 0.6% total strain tests. This is consistent with the shape of the hysteresis loops and the rapid stress relaxation during the tensile hold. The peak stresses for the 0.6% strain range were less than those observed by Rao and coworkers (1) for the continuous cycle and 600 sec hold tests by approximately 25%. Peak stresses were not reported for other hold times in the article by Rao and coworkers (1). The lower stresses observed in this work may be a result of the lower strain rate (4×10^{-3} /sec was used by Rao and coworkers (1)). It has been observed for Alloy 617 that the fatigue and creep-fatigue behavior is strongly influenced by strain rate. Differences between these data sets and the microstructural observations are discussed in more detail.

Creep-fatigue deformation is a combination of creep damage and fatigue damage and is often considered creep-fatigue when the creep and fatigue damage processes interact and accelerate the deformation process. Much of the fundamental creep-fatigue work to date has been on iron based alloys, and less on solid solution nickel based alloys. Typically three types of failure are defined: fatigue-dominated, creep-dominated, and creep-fatigue interaction. Microstructural schematics of this have been clearly illustrated by Hales (11) and Plumbridge and Ellis (12). A comprehensive summary has been written by Rodrigez and Rao (13). Fatigue dominated failures are typically observed at lower to intermediate temperatures and transgranular crack initiation and propagation is observed. On the contrary, creep dominated failures occur at high temperatures and intergranular crack initiation and propagation with extensive creep cavitation occurs. Creep-fatigue interaction (for tensile holds) is illustrated as mixed-mode crack propagation and the presence of creep cavitation on the grain boundaries in the bulk material. Cavity formation and fatigue crack initiation and propagation develop independently and then interaction occurs if one mode accelerates the other damage process. The creep and fatigue failure modes interact through cavitation accelerating the crack initiation or propagation process or fatigue deformation enhancing cavitation (13). Identifying the dominant failure mode and the influence of environment is important for life prediction and modeling efforts. Grain boundary cavitation has been observed for many alloys in the regime of creep-fatigue interaction (1, 9, 11, 13-14). A detailed assessment has correlated the size and number of grain boundary cavities and the accumulated creep damage for 316 stainless steel (11). It has also been found that a critical amount of deformation is required before creep cavities nucleate (11).

Recent work by Lillo et al. suggested that significant creep cavitation did not occur in Alloy 617 until greater than 10% creep strain during creep deformation at 900°C and 1000°C (15). In the present work, cavities were not observed in any of the creep-fatigue specimens tested at 950°C with hold times as long as 1800 sec. The total amount of creep strain accumulated during the creep-fatigue tests was estimated assuming creep did not occur in the initial stage of rapid relaxation. The creep rate observed during the hold was on the order of 10^{-7} and 10^{-8} /sec for the 0.3% and 0.6% total strain tests, respectively. This estimate suggests that less than 10% creep strain had accumulated during the test. Therefore, creep cavities are not expected to be formed in the present testing.

Interestingly, Rao and coworkers observed grain boundary cavitation and formation of wedge cracks in Alloy 617 during creep-fatigue testing at 950°C and a 0.6% total strain range that they attributed to creep damage (1). However, the testing was conducted in a simulated helium environment which produced decarburization of specimens (1). Decarburization of a creep-fatigue specimen with a 600 sec hold (total test time of 75 hours) was observed to a depth of approximately 300 μm (1). Creep cavitation and wedge cracks were observed predominately near the surface and occurred within the decarburized region. The absence of grain boundary carbides greatly enhances grain boundary sliding and thus (1) the nucleation of creep cavities and may explain their presence in creep-fatigue specimens tested in a decarburizing environment and their absence in specimens tested in an air environment. Different deformation mechanisms may result from the variations in microstructure resulting from cycling in different environments. This hypothesis will be further investigated by conducting creep-fatigue testing in various helium environments.

The creep-fatigue specimens did not fail in a fatigue-dominated manner. Intergranular initiation and propagation was observed in all of the low cycle fatigue and creep-fatigue specimens cycled at 950°C, regardless of strain range. This observation is not fully consistent with the behavior depicted by Rao and coworkers in a decarburizing helium environment (1). They reported transgranular cracking in fatigue cycled specimens ; the addition of a 60 sec tensile hold resulted in the cracking initiating transgranularly and propagating by a mixed mode (1). A large number of oxidized cracks were observed in the present creep-fatigue specimens, especially with tensile holds of greater than 600 sec. Closer examination of the specimen surface revealed that the grain boundaries were either cracked or showed precipitation of finger-like alumina (Figure 8b). Intergranular alumina precipitates are typical of air-oxidized Alloy 617: the oxygen potential at the scale/alloy interface, set by the dissociation of chromia, is very low but high enough for aluminum as well as silicon to be oxidized. Precipitation is favored at grain boundaries which are short diffusion pathways for oxygen. It is believed that the alumina veins may act as preferential sites for crack initiation. Once initiated, the cracks will open, exposing new metal surfaces to the gas phase and oxidation of the crack may occur by growth of a chromium-oxide. Eventually, the chromium oxide may

fully fill the crack, forming a large region filled with chromium oxide. Following an equivalent process, formation of intergranular alumina was observed beneath the chromium-oxide covered crack edges, in particular ahead of the crack tip, as shown in Figure 8c. Cracks are likely to propagate preferentially through these brittle alumina veins. Internal oxidation of alumina first below the surface oxide and then ahead of the crack tip may increase both crack initiation and propagation rate. This hypothesis is consistent with the observed intergranular cracking and may account for at least a portion of the reduction in the fatigue life with a tensile hold time.

Typically, grain boundary cavity nucleation is understood to accelerate crack initiation and/or propagation and through the interaction of the creep and fatigue damage processes, failure is accelerated. In the present work, transmission electron microscopy (TEM) investigation is necessary to determine the manner in which the creep damage is contributing to failure. Another factor that may be responsible for the decrease in life observed with hold time is the environment. Further work including testing in various helium environments is in progress.

CONCLUSION

Continuous cycle fatigue and creep-fatigue testing of Alloy 617 was conducted at 950°C and 0.3% and 0.6% total strain in air to simulate damage modes expected in a VHTR application. Continuous cycle and creep-fatigue specimens exhibited intergranular cracking, but did not show evidence of grain boundary cavitation. Despite the absence of grain boundary cavitation to accelerate crack propagation, the addition of a hold time at peak tensile strain was detrimental to cycle life. This suggests that creep-fatigue interaction may occur by a different mechanism or that the environment may be partially responsible for accelerating failure.

ACKNOWLEDGMENTS

The authors would like to acknowledge Joel Simpson, Randy Lloyd, Tammy Trowbridge and Todd Morris for conducting the creep-fatigue testing and metallurgical work. This work was supported through the U.S. Department of Energy Nuclear Energy.

REFERENCES

(1) Rao, K.B.S., Schiffers, H., Schuster, H. and Nickel, H. "Creep-Fatigue Interaction of Inconel 617 at 950°C in Simulated Nuclear Reactor Helium." *Metallurgical Transactions A*, 19A 359-371 (1988).

(2) Breitling, H., Dietz, W. and Penkalla, H.J. "Evaluation of Mechanical Properties of the Alloy NiCr22Co12Mo (Alloy 617) for Heat Exchanging Components of HTGRs". IWGGCR, High Temperature Metallic Materials for Gas Cooled Reactors, Cracow, Poland, 1988.

(3) Meurer, H.P., Gnirss, G.K.H., Mergler, W., Raule, G., Schuster, H. and Ullrich, G. "Investigations on the Fatigue Behavior of High-Temperature Alloys for High-Temperature Gas-Cooled Reactor Components." *Nuclear Technology*, 66 315-323 (1984).

(4) Nagato, K., Murakami, T. and Hashimoto, T. "High Temperature Low-Cycle Fatigue Strength of Hastelloy-XR". IWGGCR, High Temperature Metallic Materials for Gas Cooled Reactors, Cracow, Poland, 1989.

(5) Strizak, J.P., Cbrinkman, C.R. and Rittenhouse, P.L. "High Temperature Low-Cycle Fatigue and Tensile Properties of Hastelloy X and Alloy 617 in Air and HTGR-Helium". Specialists' Meeting on High Temperature Metallic Materials for Application in Gas Cooled Reactors, T1-T15, 1981.

(6) Tsuji, H. and Nakajima, H. "Fatigue properties of nickel-base high temperature alloys for HTGRs". *IWGGCR, High Temperature Metallic Materials for Gas Cooled Reactors*, Cracow, Poland, 1989.

(7) *ASTM Standard E606-04E1, 2004, "Standard Practice for Strain-Controlled Fatigue Testing"*. 2004.

(8) Totemeier, T. and Tian, H. "Creep-Fatigue-Environment Interactions in INCONEL 617." *Materials Science and Engineering A,* 468-470 81-87 (2007).

(9) Nagesha, A., Valsan, M., Rao, K.B.S. and Mannan, S.L. "Hold Time Effects on the Low Cycle Fatigue Behaviour of a Nimonic PE-16 Superalloy." *Trans. Indian Inst. Met.,* 53 (3), 283-290 (2000).

(10) Meurer, H., Gnirss, G., Mergler, W., Raule, G., Schuster, H. and Ullrich, G. "Investiations on the Fatigue Behavior of High-Temperature Alloys for High-Temperature Gas-Cooled Reactor Components." *Nuclear Technology,* 66 315-323 (1984).

(11) Hales, R. "A Quantitative Metallographic Assessment of Structural Degradation of Type 316 Stainless Steel During Creep-Fatigue." *Fatigue of Engineering Materials and Structures,* 3 (4), 339-356 (1980).

(12) Plumbridge, W.J. and Ellison, E.G. "Low-Cycle-Fatigue Behaviour of Superalloy Blade Materials at Elevated Temperature." *Materials Science and Technology,* 3 706-714 (1987).

(13) Rodriguez, P. and Rao, K.B.S. "Nucleation and Growth of Cracks and Cavities under Creep-Fatigue Interaction." *Progress in Materials Science,* 37 403-480 (1993).

(14) Wood, D.S., Wynn, J., Baldwin, A.B. and O'riordan, P. "Some Creep/Fatigue Properties of type 316 Steel at 625°C." *Fatigue of Engineering Materials and Structures,* 3 39-57 (1980).

(15) Lillo, T., Cole, J., Frary, M. and Schlegel, S. "Influence of Grain Boundary Character on Creep Void Formation in Alloy 617." *Metallurgical and Materials Transactions A,* 40A (12), 2803-2811 (2009).